

## ARTICLES

## ON THE DEVELOPMENT OF *LATTICE BOLTZMANN MODELING* FOR LIQUID-SOLID PHASE TRANSITIONS IN FREE SURFACE FLOWS

*Ayurzana B.<sup>1\*</sup>, Tokuzo Hosoyamada<sup>2</sup>, Tungalagtamir E.<sup>1</sup> and Batzorig G.<sup>1</sup>*

<sup>1</sup> School of Civil engineering and Architecture,  
Mongolian University of Science and Technology, Ulaanbaatar, Mongolia

<sup>2</sup> Department of Civil and Environmental Engineering,  
Nagaoka University of Technology, Nagaoka, Japan

---

ARTICLE INFO: Received: 03 Mar, 2018; Accepted: 10 Sep, 2018

---

**Abstract:** Motivated by the current lack of knowledge regarding phase transition in a free surface water flow, a novel and efficient numerical model for liquid-solid phase transition in a free surface flow has been developed for the Lattice Boltzmann Method (LBM). The proposed model consists of two physically sound modules for solving free surface flow and heat transport. The heat transport module features an immersed boundary method and a non-iterative enthalpy-based approach. Sub-cycling time integration, improving the numerical stability of the heat transport module, is introduced for the integration of modules. The performance and accuracy of the model are verified through a preliminary experiment involving a melting ice cube. The obtained results indicate that the phase transition of fluid in any flow regime can be easily handled by the model with reasonable accuracy.

**Keywords:** Free surface flow; heat transport; ice melting; immersed boundary; Lattice Boltzmann Method;

### INTRODUCTION

Phase transitions in a fluid flow, which involve both thermodynamics and hydrodynamics, are common but complex phenomena in the free-surface condition. The problems of phase transitions and free surface flow have attracted growing attention in recent years due to their importance in engineering. Moreover, these problems commonly exist simultaneously in cold nature, e.g., water

freezing or ice melting in a river, lake, ocean or a water pipe and casting in industries. However, unified numerical modeling of such problems has rarely been performed [1].

A liquid-solid phase transition problem is often referred to as a Stefan problem and basic modeling approaches have been presented in [2] and a number of other studies. Among communities conducting numerical

\*corresponding author: [ayur\\_426@yahoo.com](mailto:ayur_426@yahoo.com)

 <https://orcid.org/0000-0002-3815-1782>



The Author(s). 2018 Open access This article is distributed under the terms of the Creative Commons Attribution 4.0 International License (<https://creativecommons.org/licenses/by/4.0/>), which permits unrestricted use, distribution, and reproduction in any medium, provided you give appropriate credit to the original author(s) and the source, provide a link to the Creative Commons license, and indicate if changes were made.

studies on phase transitions by applying conventional methods, fixed spatial grid and front tracking methods are extensively used in the confined domain [3], [4] without the free-surface condition. Recent models for use in the conventional method are effective but cumbersome and require several systems of equations to solve flows and phase transitions, as well as adaptive or moving grids to clearly define melting/solidification front and iterative techniques [5] to solve nonlinear equations. However, phase transitions in a natural convection flow remain a primary focus of study. Particle-based methods, which have an inherent ability to represent the free surface, are beginning to be applied to melting and solidification problems in free surface flows [6].

In the present study, based on the advantages offered by the LBM for problems involving phase transition and the treatment of the free-surface condition, we propose a novel numerical LBM procedure for solving

the phase transition of fluid with a free surface flow.

The proposed coupled algorithm for a phase transition and free surface flow is obtained as follows: The numerical model uses two distribution functions expressed through lattices on a fixed grid: one for a flow field module and the other for a heat transport module. We slightly modified the enthalpy-based model of [7] to be non-iterative for the heat transfer, whereas phase transition was performed using the immersed boundary method with liquid fractions, which is defined by the local enthalpy. In the proposed method, the local enthalpy, obtained by iterative way in [7], is updated non-iteratively with a temperature field. We incorporated the free surface algorithm of [8] with a heat transport model.

In the following, we describe in detail the proposed method in order of numerical algorithm and numerical applications thereof.

### Lattice Boltzmann Method for free surface flows with phase transitions

#### Free surface fluid flow

The free surface algorithm for use in the LBM was first introduced by [9] and [10] for the simulation of metal foaming and was later corrected for and tested on two- and three-dimensional free surface flows by [11] and [10]. Since the free surface in the LBM can be described using the same concept applied

in the volume of fluid (VOF) method [12], each cell has a volume fraction value of fluid that is expressed as the ratio of the mass to the density of the cell, i.e.,  $\epsilon = m / \rho$ . Depending on the volume fraction value of the liquid, each cell is marked by flags as an indication of the materials in the computational cell, such as F for fluid (water), G for gas (air), S for solid, and IF for interface cells (see Fig. 1b).

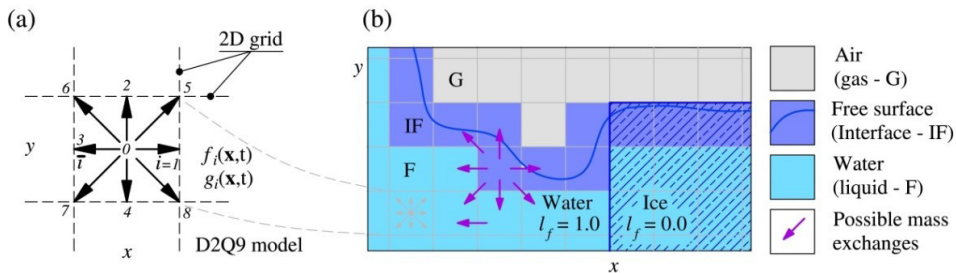


Figure 1. General scheme of the proposed model. (a) D2Q9 lattice configuration on the 2D grid; (b) materials in the domain and free surface representation.

The free surface is represented as chained single-layered interface cells, having an arbitrary volume fraction value of 0 to 1, and the evolution of the free surface is tracked by mass calculation of the interface cells and cells other than solid and gas cells, which have no

water fraction content. In contrast to the VOF method, the mass value of the cell is directly updated by mass exchange with neighboring cells at each time step of computation [8], as follows:

$$m(\mathbf{x}, t + \Delta t) = m(\mathbf{x}, t) + \sum_{i=1}^8 \Delta m_i(\mathbf{x}, t + \Delta t) \tag{1}$$

where  $\mathbf{x}$  is the space vector,  $t$  is the current time,  $\Delta t$  is the time step, and  $i$  denotes the lattice direction (Fig. 1a). Mass exchange  $\Delta m_i$  is allowed for interface cells with neighboring F or IF cells, but is not allowed for interface cells with neighboring G or S cells, as shown in Fig. 1b. Mass exchange between IF and F cells is easily defined by the difference between coming and leaving distribution functions, as  $\Delta m_i = s_e = f_i(\mathbf{x} + \mathbf{c}_i, t) - f_i(\mathbf{x}, t)$ , before the streaming step, where  $f_i(\mathbf{x})$  is a distribution function

in space and  $\mathbf{c}_i$  is a lattice velocity. After the mass is updated over the entire domain using Eq. (1), streaming and collision steps for the free surface flow module (Eq. (6)) and the heat transport module (Eq. (11)) are performed in order to obtain new macroscopic variables (Eq. (10) and Eq. (13)). Since the density of the cell is updated by Eq. (10), then the interface cell might be transformed into a G or F cell based on the following criteria:

$$\begin{aligned} IF &\rightarrow F \text{ when } m(\mathbf{x}, t + \Delta t) > (1 + k)\rho(\mathbf{x}, t + \Delta t) \text{ or} \\ IF &\rightarrow G \text{ when } m(\mathbf{x}, t + \Delta t) < (-k)\rho(\mathbf{x}, t + \Delta t), \end{aligned} \tag{2}$$

where  $k (=10^{-3})$  is the additional offset value for the emptied or filled threshold for ignoring cell, which were previously treated. Depending on the filled or emptied status of

the IF cell, the flags of neighboring G or F cells should be changed and the cells should obtain appropriate mass according to the excess mass distribution:

$$m(\mathbf{x} + \Delta t \mathbf{c}_i) = m(\mathbf{x} + \Delta t \mathbf{c}_i) + m^{ex} \left( \frac{\eta_i}{\eta_{total}} \right) \tag{3}$$

where  $m^{ex}$  is the positive or negative excess mass of the filled or emptied IF cell, and  $\eta_{total}$  is the sum of all weights  $\eta_i$ , each of which

is computed by normal vector  $\mathbf{n}$  on the free surface as follows:

$$\begin{aligned} \eta_i &= \begin{cases} \mathbf{n} \cdot \mathbf{c}_i & \text{if } \mathbf{n} \cdot \mathbf{c}_i > 0 \\ 0 & \text{otherwise} \end{cases} \text{ for filled cells, and} \\ \eta_i &= \begin{cases} -\mathbf{n} \cdot \mathbf{c}_i & \text{if } \mathbf{n} \cdot \mathbf{c}_i < 0 \\ 0 & \text{otherwise} \end{cases} \text{ for emptied cells.} \end{aligned} \tag{4}$$

Actually, the flags of the changed cells, i.e., the emptied or filled IF cells and their neighboring G or F cells, are not allowed to change before the excess mass is distributed. Based on Eq. (2), these cells will have a temporal transition flag during the excess

mass distribution. Moreover, the distribution functions of the newly generated interface cells having temporal transition flags, which changed from G to IF, can be initialized with the equilibrium distribution functions.

Right after the streaming step in the

fluid flow module, the free surface boundary condition must be imposed on the interface cells in order to recover the distribution functions that would be streamed from G cells.

The free surface boundary condition assumes that the fluid has a much lower kinematic viscosity than the gas state [8] and is expressed in terms of the following distribution function:

$$f_i'(\mathbf{x}, t + \Delta t) = f_i^{eq}(\rho_A, \mathbf{u}) + f_i^{eq}(\rho_A, \mathbf{u}) - f_i(\mathbf{x}, t) \tag{5}$$

where  $\rho_A$  is the gas density implicitly acting as air pressure on the free surface and the velocity  $\mathbf{u}$  is defined by using Eq. (10) in previous time step or by initial condition at first.

are available for the time evolution of the distribution function by the discretized *Lattice Boltzmann* equation with the Bhatnagar-Gross-Krook (BGK) collision operator [13] and modification of the immersed moving boundary [14]:

$$f_i(\mathbf{x} + \mathbf{c}_i \Delta t, t + \Delta t) - f_i(\mathbf{x}, t) = -\frac{\Delta t(1 - \beta)}{\tau_{tot}} (f_i(\mathbf{x}, t) - f_i^{eq}(\mathbf{x}, t)) + \beta f_i^m(\mathbf{x}, t) + \Delta t F_i, \tag{6}$$

where  $\mathbf{c}_i$  is the discrete unit velocity in the  $i$  direction,  $\tau_{tot}$  is the dimensionless relaxation time with respect to the lattice viscosity  $\nu$  and

is adjusted with the sub-grid scale turbulent model proposed by [15], and  $\beta$  is the parameter given by [16]

$$\beta(l_f, \tau) = \frac{(1 - l_f)(\tau - 0.5)}{l_f + (\tau - 0.5)}, \tag{7}$$

in which  $l_f(\mathbf{x}, t)$  is the liquid fraction value of the cell, which takes a value between 0 and 1. Liquid fraction values of 0 and 1 represent ice and water, respectively, as shown in Fig. 1b. In Eq. (7), the total relaxation  $\tau_{tot}$  can be used instead of the relaxation time  $\tau$ . The immersed boundary modification can be used for not only dynamic separation of solid (ice) and liquid (water) phases, but also for a moving body (moving ice) in a fluid flow

[17]. In this regard, freely moving ice and its melting process have been successfully tested with the experimental results [17]. Dynamic interface between the liquid and solid states in phase transition phenomena is considered as a complicated moving boundary problem. Therefore, an additional collision term  $f_i^m$ , which easily handles the moving boundary, is for cells partially or fully covered by a solid, i.e., ice cell, is given as

$$f_i^m(\mathbf{x}, t) = f_i(\mathbf{x}, t) - f_i(\mathbf{x}, t) + f_i^{eq}(\rho, \mathbf{u}_s) - f_i^{eq}(\rho, \mathbf{u}), \tag{8}$$

where  $\mathbf{u}_s$  is the velocity of the moving solid, which is set to 0 in the present study, i.e., the

ice is fixed. In Eq. (6), we use the force scheme proposed by [18] for the body force term:

$$F_i = w_i \left( 1 - \frac{1}{2\tau_{tot}} \right) \left[ \frac{\mathbf{c}_i - \mathbf{u}}{c_s^2} + \frac{\mathbf{c}_i(\mathbf{c}_i \cdot \mathbf{u})}{c_s^4} \right] \cdot \mathbf{F} \text{ with } \mathbf{F} = \mathbf{g}(1 - \alpha_v(\theta - \theta_o)^2) \tag{9}$$

where  $\mathbf{g}$  is the dimensionless acceleration due to gravity,  $\alpha_v$  is the thermal volume expansion of water, and  $\theta_o$  is the dimensionless reference

temperature at the maximum density of water. The value of  $\mathbf{g}$   $\alpha_v$  can be defined in terms of the Rayleigh number (Ra) definition. The force  $\mathbf{F}$  in

Eq. (9) includes the acceleration of gravity and non-Boussinesq approximation [19] and [17] for the buoyance. The equilibrium distribution function for an incompressible fluid flow can be determined by the expansion of a Maxwell

$$\rho = \sum_{i=0}^8 f_i, \quad \rho \mathbf{u} = \sum_{i=0}^8 \mathbf{c}_i f_i + \frac{\mathbf{F} \Delta t}{2}. \tag{10}$$

In the free surface LBM, the simulation neglects G and S cells [21] in order to reduce the computational time, because these cells are

distribution [20]. The macroscopic variables, namely density  $\rho$  and velocity  $\mathbf{u}$ , can be computed based on the order of the moments of the distribution functions  $f_s$  as

only involved in the imposition of the boundary conditions, and so no physical variables will be determined in the gas phase.

*Heat transfer with phase transition in LBM*

In the modeling of heat transport with phase transition, the temperature field is considered to be an essential variable and can be calculated

by the following thermal Lattice Boltzmann equation with latent heat of fusion [22]:

$$g_i(\mathbf{x} + \mathbf{c}_i \Delta t, t + \Delta t) - g_i(\mathbf{x}, t) = -\frac{(g_i(\mathbf{x}, t) - g_i^{eq}(\mathbf{x}, t))}{\tau_h} - w_i \frac{L_h}{c_p} (l_f(\mathbf{x}, t - \Delta t) - l_f(\mathbf{x}, t)), \tag{11}$$

where  $g_i(\mathbf{x}, t)$  is the distribution function for the temperature field,  $\tau_h (= 3\alpha + 1/2)$  is the dimensionless relaxation time with respect to the thermal diffusivity  $\alpha$ ,  $L_h$  is the dimensionless latent heat of fusion, and

$c_p$  is the specific heat capacity of water or ice. The specific heat capacity and thermal diffusivity must be defined appropriately on the computational cell depending on the cell

$$\alpha = (1 - l_f(\mathbf{x})) \alpha^{ice} + l_f(\mathbf{x}) \alpha^{water} \text{ and}$$

$$c_p = (1 - l_f(\mathbf{x})) c_p^{ice} + l_f(\mathbf{x}) c_p^{water}, \tag{12}$$

where the superscripts <sup>ice</sup> and <sup>water</sup> indicate the thermal diffusivities and specific heat capacities of ice and water, respectively. The specific heat capacity of water in lattice form can be obtained from the Stefan number,  $St = (c_p^{water} \Delta \theta) / L_h$ , and is

related to the specific heat capacity of ice as  $c_p^{R-ice} / c_p^{R-water} = c_p^{ice} / c_p^{water}$ . The Stefan number in the simulations of the present study is always fixed at 0.5. The equilibrium distribution function for the temperature field can be given as

$$g_i^{eq} = w_i \theta \left[ 1 + \frac{\mathbf{c}_i \cdot \mathbf{u}}{c_s^2} \right] \text{ with } \theta = \sum_{i=0}^8 g_i, \tag{13}$$

and the macroscopic temperature  $T$  can be converted into dimensionless temperature  $\theta$  as follows:

$$T = \frac{T_{max} - T_{melt}}{\theta_{max} - \theta_{melt}} (\theta - \theta_{melt}) + T_{melt} . \tag{14}$$

After the dimensionless temperature evolution,  $\Delta t)L_h$ , can be used to linearly interpolate the the local enthalpy, obtained by  $En=c_p \theta + l_f(x,t-$  liquid fraction,

$$l_f(x) = \begin{cases} 1 & \text{for } En > En_s + L_h = En_l \\ 0 & \text{for } En < En_s = c_p \theta_{melt} \\ \frac{En - En_s}{En_l - En_s} & \text{for } En_s \leq En \leq En_s + L_h \end{cases} , \tag{15}$$

and the liquid fraction defines the liquid (water) and solid (ice) phases in the domain. The model does not require iteration for the local enthalpy, since it was reported that the enthalpy update without iteration has negligible effects [7]. And also the model uses exact thermal properties for phases, which are often neglected in existing numerical methods, i.e., the thermal properties of the

liquid are used for both the solid and liquid phases. Numerically, Eq. (6) and (11) must be solved in two steps, namely the collision and streaming steps.

The multiscale expansion, the so-called *Chapman-Enskog* expansion [20], of Eq. (6) without the immersed boundary modification gives the following dimensionless macroscopic equation in summation convention:

$$\frac{\partial \rho}{\partial t} + \frac{\partial(\rho u_\alpha)}{\partial x_\alpha} = 0 \text{ and} \tag{16}$$

$$\frac{\partial(\rho u_\alpha)}{\partial t} + \frac{\partial(\rho u_\alpha u_\beta)}{\partial x_\beta} = -\frac{\partial \rho}{\partial x_\alpha} c_s^2 \delta_{\alpha\beta} + \left(\frac{\Delta t}{w} - \frac{\Delta t}{2}\right) c_s^2 \frac{\partial^2(\rho u_\alpha)}{\partial x_\beta^2} + \rho F_\alpha , \tag{17}$$

where the viscosity is identified as

$$\nu = \Delta t \left( \tau_\nu - \frac{1}{2} \right) c_s^2 , \tag{18}$$

as the continuity and momentum equations, respectively. The immersed boundary modification, which is realized as the bounce-back rule for the non-equilibrium part of the distribution functions [14], in the multiscale expansion will lead the form of a forcing

function in Eq. (17) that reproduces the effect of the immersed boundary [23]. For the heat transfer module, equation (11) can recover the following dimensionless macroscopic equation using the multiscale expansion:

$$\frac{\partial \theta}{\partial t} + u_\alpha \frac{\partial \theta}{\partial x_\alpha} = c_s^2 \left( \tau_h - \frac{\Delta t}{2} \right) \frac{\partial^2 \theta}{\partial x_\alpha^2} - \frac{L_h}{c_p} \frac{\partial l_f}{\partial t} \tag{19}$$

where the heat source term,  $\frac{L_h}{c_p} \frac{\partial l_f}{\partial t}$ , is directly derived from the last term in the right hand side of Eq. (11) [22].

*Implementation*

The computation is performed only for F and IF cells with the free surface algorithm, and G or S cells must be used to impose a boundary condition on the free surface or solid walls. The phase, i.e., ice or water, is assigned to F cells (Fig. 1b) because ice, which acts like a solid, will become water after melting. Moreover, if ice interacts with the air (G cells), boundary cells between the ice and air must be IF cells because IF cells have a certain water content. At the interface between ice and water,  $n_s$  takes a value of between 0 and 1, where a “mushy” zone [24] may be observed when conduction dominates heat transfer [25] and can be defined when the solidus and liquidus temperature are distinguished [22]. The interaction between

$$n_s = \left\lfloor \frac{\Delta t_h}{\Delta t_f} \right\rfloor + 1, \tag{25}$$

where  $\lfloor \cdot \rfloor$  is the floor operator to convert a real number to an integer,  $\Delta t_h$  is the time step of the

the free surface flow module and the heat transport with phase change module is such that the temperature difference produces a buoyance force in the flow field, and the flow field affected by the buoyance force forms a temperature field in the domain. Although the buoyance force is negligible in a turbulent flow, it must be included in the computation. The lattice viscosity is related to the lattice thermal diffusivity of a fluid as  $\alpha^{water} = \nu / Pr$ , where  $Pr$  is the Prandtl number, so that the relation between the computational modules is maintained. However, depending on the choice of grid spacing and time step, the modules must be integrated in two different time scales, which results in sub-cycling in the time integration, as follows:

heat transport module, and  $\Delta t_f$  is the time step of the fluid flow module.

**Model development and validations**

In a previous study [25], we successfully solved the natural convection flow in order to validate the numerical code of a fluid flow with heat transport. The validated code was then

extended to include a phase transition without the latent heat source term. With the following tests, the validity of the proposed model is elaborated.

*Melting of a slab of ice*

Here we consider a Stefan problem, melting of a slab of ice with length of 0.1 m, to validate

the proposed *Lattice Boltzmann* Method. The analytical solution of this problem is given as [2]

$$X(t) = 2\chi \sqrt{\alpha_R^{water} t} \text{ and} \tag{20}$$

$$T(x, t) = T_{max} - (T_{max} - T_{melt}) \frac{\text{erf}\left(x/2\sqrt{\alpha_R^{water} t}\right)}{\text{erf}(\chi)} \tag{21}$$

with the transcendence function for  $\chi$ ,

$$\chi e^{\chi^2} \text{erf}(\chi) = \frac{St}{\sqrt{\pi}}, \tag{22}$$

to find positions of liquid-solid interface and temperature distributions in liquid region at

times, respectively. Initially, temperature of the ice slab was at melting temperature of

$T_{melt} = 0^{\circ}C$ . One side of the ice was insulated, while the other was set at  $T_{max} = 25^{\circ}C$  abruptly at  $t=0$  and it is maintained for all times  $t>0$  in our experiment. We set imaginary thermocouples in the slab at a length of 0.01, 0.03, 0.05, and 0.09 m respectively and measured the

temperature in time evolution. Simply, we chose 100 grids for the length of the slab in both the analytical and numerical solutions. For the numerical solution, we used D1Q3 lattice arrangement [26] for Eq. (16) and the relaxation time is obtained from the relation

$$\tau_h = 3\alpha_R^{water} \frac{\Delta t_h}{\Delta x^2} + 0.5, \tag{23}$$

where  $\Delta t_h$  is the time step, which is set as  $\Delta t_h = 0.1 s$  and  $\Delta x (= 0.001 m)$  is the grid spacing. The constant temperature boundary condition [27] is applied for the heated side of the slab, while the second order extrapolation boundary condition [26] is imposed on the other side. The temperature is calculated by Eq. (14) using the dimensionless temperature computed by LBM, and then the melting front, the liquid-solid interface, is defined by the liquid fraction value using Eq. (15).

The total melting time was defined as 34.01 hours by the analytical and the present LBM (1). The comparisons of the results by the analytical and numerical solutions are given in Figs. 2 and 3. The colour map of Fig. 2 is the temperature distribution estimated by the analytical solution. The result of the present LBM (1) uses the relaxation time defined by Eq. (23), whereas the LBM (2) uses the adjusted relaxation time, where the thermal diffusivity is considered as a function of temperature. The good fit of the melting fronts is found

between the analytical solution and the LBM (2) because the simulation takes advantage of the more proper value of thermal diffusivity for the given range of temperature. However, the total melting time with the LBM (2) lasted 34.29 hours. The numerically defined melting fronts in Fig. 2, as well as the temperature profiles at different times and measurement positions in Fig. 3, show the discrepancy in the middle of the simulation time. Good agreement is observed before 8.5 hours and after 30 hours in the experiment, as shown in Figs. 2 and 3. The temperature profiles at specific times, which are the times the melting front reaches the imaginary thermocouples, by the analytical solution, show the linear in space, while the profiles defined by the LBM show the deviation in space. The maximum errors of the LBM compared to the analytical solution are reported in Table 1. The Stefan problem gives the validation for phase transition of ice in tiny volume ignoring the fluid flow, as well as the free-surface condition.

Table 1. Maximum errors of LBM compared to analytical solution

Cases	Relaxation time, $\tau_h$	Maximum error (%)		
		of melting front	of temperature profiles at times	of temperature profiles at positions
LBM (1)	0.579	4.04	5.59	5.00
LBM (2)	0.569	1.32	7.80	4.53

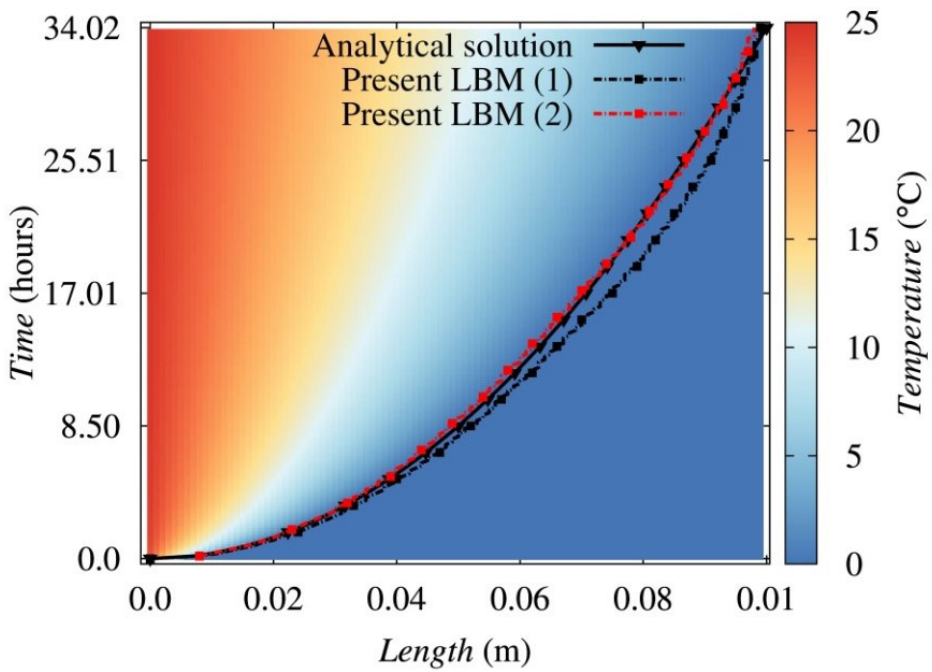


Figure 2. Time history of temperature distribution and melting front locations by the analytical and numerical methods.

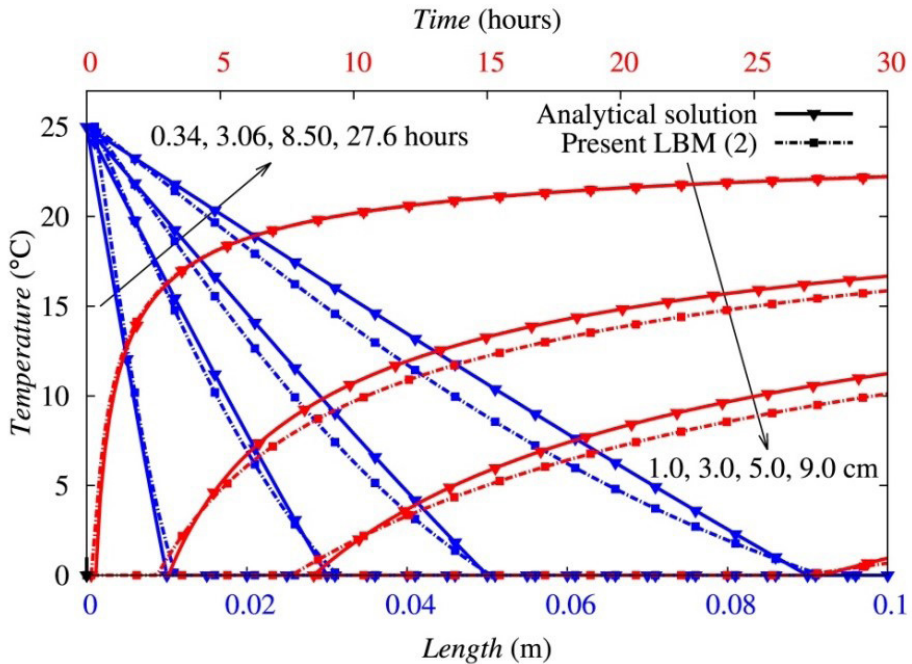


Figure 3. Temperature profiles at different times and at different positions: blue lines for the temperature distributions at times and red lines for the temperature distributions at positions.

*Melting of an ice cube in ambient temperature*

In order to validate the proposed numerical procedure in the free-surface condition, we carried out a brief laboratory experiment. The melting of an ice cube prepared in a freezer was compared with the results of LBM simulation. We used a commercially available infrared thermal imaging camera to measure the temperature distribution in a captured frame. An ice cube having sides of 4.5 cm was placed on a smooth wooden surface having lower thermal diffusivity and lower reflection of heat. In the heat transport module of the numerical model, the wooden surface was modeled as an adiabatic wall and the constant-temperature boundary condition was imposed on the water/ice surface interacting with the surrounding air. The temperature was maintained constant at room temperature on

the boundary, as in experiment. In the fluid flow module, the wooden surface under the ice cube was assumed to be a no-slip wall, whereas the free surface boundary condition (Eq. (5)) without surface tension was assumed for the water/ice surface interacting with the air. We used 60 grids for one side of the ice cube, the grid spacing was  $\Delta x = 7.5 \times 10^{-4} \text{ m}$ , and the time steps were  $\Delta t_f = 6.91 \times 10^{-3} \text{ s}$  and  $\Delta t_h = 7.603 \times 10^{-2} \text{ s}$ . These time steps provided sub-cycling at  $n_s = 12$ , so that the heat transport module is performed once every twelve steps of the fluid flow module. The time sequence of the thermal image is shown in Fig. 4a, followed by the corresponding numerical results in Figs. 4b and 4c. In the experiment, ice melts from the bottom at a low rate, although no melting occurs in numerical simulation because of the given boundary condition.

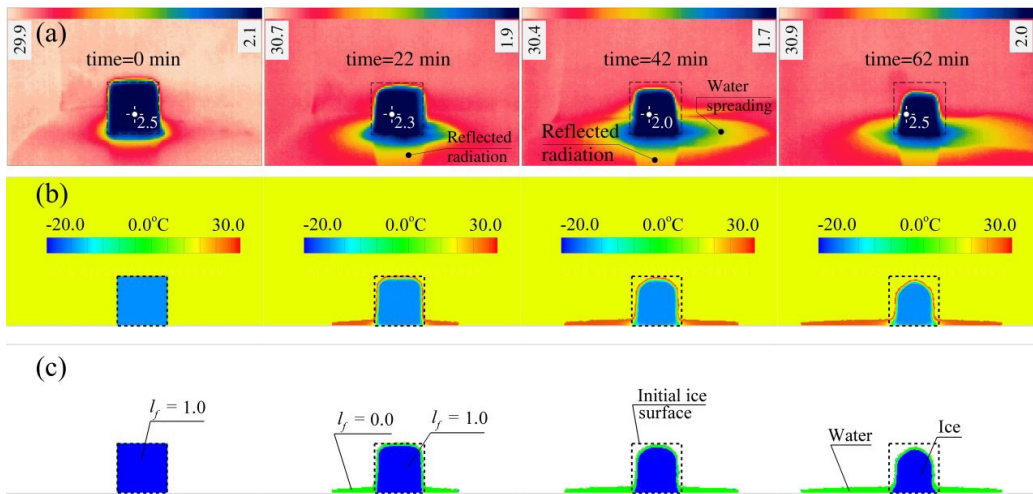


Figure 4. Time sequences of the experimental and numerical results for an ice cube melting in ambient air. (a) Infrared images of the ice cube and ambient condition; (b) numerically determined temperature field; (c) numerically determined ice and water phases.

As shown in Fig. 4, the difference in height of the melting ice cube after 62 min was 3.56 mm, whereas the numerical value was higher. The top of the ice cube became rounded in the numerical simulation, whereas, in experimental test, the top remained approximately flat. The reason for this difference in shape might be related to the velocity of flowing water on the surface of the ice cube. The water thickness

flowing on the ice surface in the numerical test, indicated as  $l_f = 0$  in Fig. 4c, was observed to be much thicker than in the experiment. Since we used a coarse grid for discretization, the numerical model requires at least two double-layer grids to simulate the surface of the water covering the ice. The average water surface temperature on the ice, as determined by the thermal camera, was approximately

2.2°C in the experiment, as shown in Fig. 4a, which agreed with the result of the numerical simulation for the ice-water interface. For the sake of generality, we show the remaining ice percentage with respect to melting time in Fig. 5, which shows the accuracy of the numerical model. The melting rate of ice was nearly linear, and the numerical results were

in good agreement with the experiment results, with the exception of the initial oscillation in the numerical results. Similar studies were conducted by [28] for an ice cube in still water and by [29] for an ice cube melting in ambient air. Both of these studies used particle-based methods, and their results were less continuous and exhibited a step-like tendency over time.

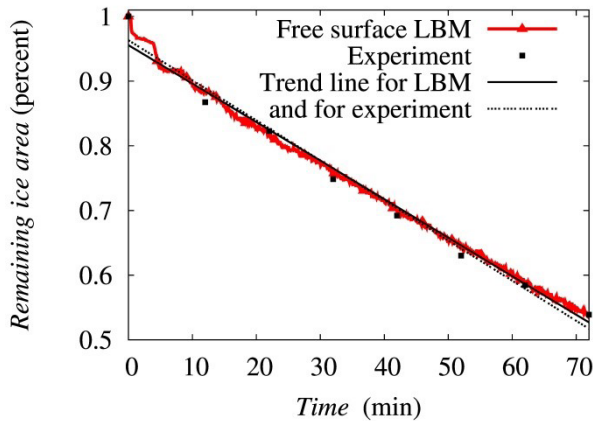


Figure 5. Experimentally and numerically determined remaining ice area.

## CONCLUSIONS

The phase transition of water in free surface flow was numerically modeled in a framework of the *Lattice Boltzmann Method*. The novel computational model includes modules that take into account heat transport with phase transition and free surface fluid flow and liquid-solid phase transition treatment by the immersed boundary modification into the *Lattice Boltzmann equation*. The proposed model uses appropriate thermal properties, namely, thermal diffusivity and specific heat capacity, for the ice and water phases, so that heat transport can be properly defined in each phase. The modules in the model incorporate sub-cycling of time integration, which

effectively improves the numerical stability in computation. Based on numerical analysis, the numerical model was proved to be acceptable for use in engineering research in terms of numerical consistency.

Several improvements and additions to the proposed model are being considered as areas for future research. For instance, the model performance for freezing or ice formation study must be properly tested and validated through experimental studies under various conditions. Also, the modeling of freely moving ice that is melting or freezing is a challenge [17]. However, the present paper has laid the foundation for these improvements.

## REFERENCES

- [1] S. Fukusako and M. Yamada, "Recent advances in research on water-freezing and ice-melting problems," *Experimental Thermal and Fluid Science*, vol. 6, no. 1, pp. 90-105, 1993.
- [2] V. Alexiades, *Mathematical modeling of melting and freezing processes.*, CRC Press, 1992.
- [3] H. Hu and S. A. Argyropoulos, "Mathematical modelling of solidification and melting: a review," *Modelling and Simulation in Materials Science and Engineering*, vol. 4, no. 4, p. 371, 1996.
- [4] Z. Virag, M. Živić and A. Galović, "Influence of natural convection on the melting of ice block surrounded by water on all sides," *Int. J. of heat and mass transfer*, vol. 49, no. 21, pp. 4106-4115, 2006.
- [5] I. Danaila, R. Moglan, F. Hecht and S. Le Masson, "A Newton method with adaptive finite elements for solving phase-change problems with natural convection," *Journal of Computational Physics*, vol. 274, pp. 826-840, 2014.
- [6] K. Iwasaki, H. Uchida, Y. Dobashi and T. Nishita, "Fast Particle-based Visual Simulation of Ice Melting," in *Computer Graphics Forum, Vol.29, No. 7, pp.2215-2223*, Blackwell Publishing Ltd, 2010.
- [7] C. Huber, A. Parmigiani, B. Chopard, M. Manga and O. Bachmann, "Lattice Boltzmann model for melting with natural convection," *Int. J. of Heat and Fluid Flow*, vol. 29, no. 5, pp. 1469-1480, 2008.
- [8] C. Körner, M. Thies, T. Hofmann, N. Thürey and U. Råde, "Lattice Boltzmann model for free surface flow for modeling foaming," *Journal of Statistical Physics*, vol. 121, no. 1-2, pp. 179-196, 2005.
- [9] C. Körner and R. F. Singer, "Processing of metal foams—challenges and opportunities," *Advanced Engineering Materials*, vol. 2, no. 4, pp. 159-165, 2000.
- [10] N. Thürey, C. Körner and U. Råde, "Interactive free surface fluids with the lattice Boltzmann method," Technical Report 05-4. University of Erlangen-Nuremberg, Germany, 2005.
- [11] N. Thürey, *Physically Based Animation of Free Surface Flows with the Lattice Boltzmann Method*, Nuremberg: Verlag Dr. Hut., 2007.
- [12] C. W. Hirt and B. D. Nichols, "Volume of fluid (VOF) method for the dynamics of free boundaries," *Journal of computational physics*, vol. 39, no. 1, pp. 201-225, 1981.
- [13] P. L. Bhatnagar, E. P. Gross and M. Krook, "A model for collision processes in gases. I. Small amplitude processes in charged and neutral one-component systems," *Physical review*, vol. 94, no. 3, p. 551, 1954.

- [14] D. R. Noble and J. R. Torczynski, "A lattice-Boltzmann method for partially saturated computational cells," *International Journal of Modern Physics C*, vol. 9, no. 08, pp. 1189-1201, 1998.
- [15] S. Hou, J. Sterling, S. Chen and G. D. Doolen, "A lattice Boltzmann subgrid model for high Reynolds number flows," *arXiv preprint comp-gas/9401004*, 1994.
- [16] O. E. Strack and B. K. Cook, "Three-dimensional immersed boundary conditions for moving solids in the lattice-Boltzmann method," *Int. J. for Numerical Methods in Fluids*, vol. 55, no. 2, pp. 103-125, 2007.
- [17] A. Badarch and H. Tokuzo, "Lattice Boltzmann Method for the Numerical Simulations of the Melting and Floating of Ice," in *Free Surface Flows and Transport Processes (pp. 143-154)*. Springer, Jachranka, 2018.
- [18] Z. Guo, C. Zheng and B. Shi, "Discrete lattice effects on the forcing term in the lattice Boltzmann method," *Physical Review E*, vol. 64, no. 4, p. 046308, 2002.
- [19] W. Tong and J. N. Koster, "Natural convection of water in a rectangular cavity including density inversion," *International journal of heat and fluid flow*, vol. 14, no. 4, pp. 366-375, 1993.
- [20] Z. Guo and C. Shu, *Lattice Boltzmann method and its applications in engineering (Vol.3)*, World Scientific, 2013.
- [21] B. Ayürzana, T. Hosoyamada and T. Nasanbayar, "Hydraulics application of the Free-surface Lattice Boltzmann method," in *Proceeding of IFOST-2016, 11(2), 195-199*, Novosibirsk, 2016.
- [22] W. S. Jiaung, J. R. Ho and C. P. Kuo, "Lattice Boltzmann method for the heat conduction problem with phase change," *Numerical Heat Transfer: Part B: Fundamentals*, vol. 39, no. 2, pp. 167-187, 2001.
- [23] R. Mittal and G. Iaccarino, "Immersed boundary methods," *Annu. Rev. Fluid Mech.*, vol. 37, pp. 239-261, 2005.
- [24] V. R. Voller and C. Prakash, "A fixed grid numerical modelling methodology for convection-diffusion mushy region phase-change problems," *Int. J. of Heat and Mass Transfer*, vol. 30, no. 8, pp. 1709-1719, 1987.
- [25] B. Ayürzana and T. Hosoyamada, "Phase change simulations of water near its density inversion point by Lattice Boltzmann method," in *Proceedings of the 23rd IAHR Int. Sym. on Ice*, Ann Arbor, 2016.
- [26] A. A. Mohamad, *Lattice Boltzmann Method: fundamentals and engineering applications with computer codes*, Springer Science & Business Media, 2011.
- [27] A. A. Alamyane and A. A. Mohamad, "Simulation of forced convection in a channel with extended surfaces by the lattice Boltzmann method," *Computers & Mathematics with Applications*, vol. 59, no. 7, pp. 2421-2430, 2010.

- [28] F. Faizal and R. R. Septiawan, “Computational Study on Melting Process Using Smoothed Particle Hydrodynamics,” *Journal of Modern Physics*, vol. 5, no. 03, p. 112, 2011.
- [29] D. S. Tan, “Modelling Melting Ice using the Smooth Dissipative Particle Dynamics Method,” in *19th Australasian Fluid Mechanics Conference*, 2014.